Encapsulation and controlled release of rapamycin from polycaprolactone nanoparticles prepared by membrane micromixing combined with antisolvent precipitation

Rahimah Othman[†,‡,*], Goran T. Vladisavljević[†,*], Zoltan K. Nagy[†,§], R.G. Holdich[†]

[†]Department of Chemical Engineering, Loughborough University, Ashby Road, Loughborough, Leicestershire LE11 3TU, UK

[‡]School of Bioprocess Engineering, Universiti Malaysia Perlis, Kompleks Pusat Pengajian Jejawi 3, 02600 Arau, Perlis, Malaysia

[§]School of Chemical Engineering, Purdue University, West Lafayette, IN 47907-2100, USA

KEYWORDS: Rapamycin, Nanoparticles, Membrane Micromixing, Precipitation, Controlled Drug Release

ABSTRACT: Rapamycin loaded polycaprolactone nanoparticles (RAPA-PCL NPs) with a polydispersity index of 0.006–0.073 were fabricated by anti-solvent precipitation combined with micromixing using a ringed stainless steel membrane with 10-μm diameter laser-drilled pores. The organic phase composed of 6 g L^{-1} of PCL and 0.6–3.0 g L^{-1} of RAPA in acetone was injected through the membrane at 140 L m^{-2} h^{-1} into 0.2 wt% aqueous polyvinyl alcohol solution stirred at 1300 rpm, resulting in a Z-average mean of 189–218 nm, a drug encapsulation efficiency of 98.8–98.9 % and a drug loading in the NPs of 9–33 %. The encapsulation of RAPA was confirmed by UV-Vis spectroscopy, XRD, DSC, and ATR-FTIR. The disappearance of sharp characteristic peaks of crystalline RAPA in the XRD pattern of RAPA-PCL NPs revealed that the drug was molecularly dispersed in the polymer matrix or RAPA and PCL were present in individual amorphous domains. The rate of drug release in pure water was negligible due to low aqueous solubility of RAPA. RAPA-PCL NPs released more than 91 % of their drug cargo after 2.5 h in the release medium composed of 0.78–1.5 M of the hydrotropic agent N,N-diethylnicotinamide, 10 vol% of ethanol, and 2 vol% of Tween 20 in phosphate buffered saline. The dissolution of RAPA was slower when the drug was embedded in the PCL matrix of the NPs than dispersed in the form of pure RAPA nanocrystals.

Introduction

Rapid progress in nanomedicine has led to the development of new drug delivery strategies for poorly water-soluble drugs that can overcome their instability and poor bioavailability.[1] Nanovehicles such as micelles, liposomes, dendrimers, quantum dots, carbon nanotubes, nanogels, polymeric nanospheres, solid lipid nanoparticles (NPs), and inorganic NPs offer increased longevity in the blood, enhanced intracellular penetration, site-specific targeting, in vivo visualization, and stimuli responsiveness.[2,3] Polymeric NPs composed of poly(lactide-co-glycolide) (PLGA), poly(D,L-lactide) (PDLLA), poly(ε-caprolactone) (PCL), and poly(alkyl cyanoacrylates) (PACs) are especially popular due to their controlled/sustained release properties, biocompatibility (non-toxic, non-immunogenic, and non-inflammatory properties), and applicability to many water insoluble drugs.[4] Polymeric NPs can be prepared by antisolvent precipitation, which is less energy demanding and more facile method than emulsion-solvent evaporation and applicable without any additives in the aqueous phase.[5–7]

Rapamycin (RAPA) or sirolimus is a carboxylic lactone-lactam macrolide with antifungal, antitumor, anti-inflammatory, and immunosuppressive properties, first isolated in 1975 from Streptomyces hygroscopicus. [8] Clinical applications of RAPA for breast cancer therapy and prevention of restenosis after coronary stent placement was impeded by its poor solubility in water (2.6 μg·mL^{-1} at 25 °C), low bioavailability, dose-limiting toxicity,[9] and low stability in plasma and low- and neutral-pH buffers with a half-life of less than 10 h at 37 °C.[8] To improve oral bioavailability of RAPA, various biodegradable polymeric NPs with hydrophobic cores have been developed to solubilise RAPA and protect it against degradation after administration. RAPA-loaded PLGA, PCL-poly(ethylene glycol) (PEG)-PCL, PDLLA, poly(ethylene oxide) (PEO)-PLGA, and mPEG-b-PLA NPs were prepared using a modified nanoprecipitation technique,[10] emulsion-solvent evaporation method, [9,11–14] and the salting-out method.[15] RAPA-loaded chitosan/PLA NPs have been prepared by ultrasonic-assisted nanoprecipitation,[16] but the process does not lead to narrow particle size distribution.

Control over the size of drug-loaded NPs is critically important to avoid particle uptake by the reticuloendothelial system and maximise their accumulation in tumour sites by exploiting the enhanced retention and permeability (EPR) effect. The optimal size of NPs for achieving the EPR effect depends on the tumour type, location and size, and the maximum NP size is usually 380–780 nm.[17] Size-tuneable NPs can be prepared by nanoprecipitation/micromixing using microporous membrane[18,19] or microfluidic channels.[20,21]

In membrane micromixing, the organic phase is introduced into the aqueous phase through a microporous membrane under controlled injection rate and shear on the membrane/aqueous phase interface. Here, the role of membrane is to uniformly split the organic phase stream into numerous microstreams, allowing for more uniform mixing conditions compared to direct injection through a single injection point, e.g. via a hypodermic needle. Membranes commonly used in this process are composed of a random network of irregular pores with a wide distribution of pore sizes, such as ceramic,[22] polymeric hollow fibre,[23] and Shirasu Porous Glass[24] membrane. These membranes contain tortuous and interconnected pores, which make them difficult to clean, and exhibit high flow resistance due to significant thickness. Recently, isoporous microengineered membranes with ordered pore arrays have been used to prepare emulsions[25] and micro/nano-particles.[26,27] Such membranes have a low flow resistance and low tendency for fouling, due to their small thickness and non-interconnected, straight-through pores.[28] Microengineered membrane was mainly used in a simple stirred cell, but scalable continuous systems have also been developed, based on pulsed back-and-forward cross flow[29] and oscillating membrane with either upward and downward[30] or clockwise and counterclockwise[31] motion.

In this work, novel RAPA-loaded PCL NPs (hereafter abbreviated as RAPA-PCL NPs) with a narrow size distribution have been facilely produced by antisolvent precipitation using ringed stainless steel (SS) membrane fabricated by pulsed laser micromachining. This fabrication process leads to cylindrical pores that are less prone to fouling and provide more efficient mixing than funnel-shaped pores of electroformed nickel membrane.[32] The main objective of this work were to investigate the effect of incorporation of RAPA in the polymer matrix on the physicochemical properties of the produced NPs and to study the encapsulation efficiency of RAPA inside the NPs and their in vitro drug release behavior in different release media. PCL is a FDA-approved biodegradable drug carrier, selected due to its suitability for the encapsulation of poorly water-soluble drugs and its negligible tendency to generate an acidic environment during degradation, which can lead to inflammatory reactions in the body.[33,34]

Materials and Methods

Materials. Poly(ε-caprolactone) (PCL, Mw = 14,000 kDa with a glass transition temperature of 60 °C), tetrahydrofuran (THF, HPLC grade, purity ≥ 99.9 %), and polyvinyl alcohol (PVA, M_w = 13–23 kDa, 87-89 % hydrolysed) were purchased from Sigma-Aldrich (Dorset, UK). PVA was used as a water soluble stabiliser to prevent agglomeration, coalescence and imperfect surface formation of the NPs. Acetone, (Ace, HPLC grade, purity ≥ 99.8 %), acetonitrile (HPLC grade, purity ≥ 99.9 %), methanol (HPLC grade, purity ≥ 99.8 %), acetic acid (HPLC grade, purity ≥ 99.7 %), and N,N-diethylnicotinamide (DENA, 97 %, Acros Organics BVBA) were purchased from Fisher Scientific Ltd (Loughborough, UK). Rapamycin (RAPA, sirolimus, purity ≥ 99 %) was provided by Chunghwa Chemical Synthesis & Biotech Co. Ltd. (New Taipei City, Taiwan). All chemicals were of analytical grade. For RAPA-PCL NPs, the organic phase was prepared by dissolving 0.6–3.0 g L^{-1} of RAPA and 6 g L^{-1} of PCL in acetone. For production of RAPA nanocrystals, the organic phase was composed of 0.3 wt% RAPA in acetone, whilst for blank PCL NPs the organic phase was prepared by dissolving 1 g L^{-1} of PCL in THF or acetone. In all experiments, the aqueous phase was 0.2 wt% PVA solution prepared in Milli-Q water.

Membrane and membrane module. The stirred cell used in this work was equipped with a flat SS membrane placed under a paddle blade stirrer, as shown in Figure 1a. Both the cell device and membrane were supplied by Micropore Technologies Ltd (Redcar, UK). The membrane had 6,912 pores with a diameter of 10 μm fabricated by laser drilling within an annular region with a surface area of 2.76 cm^2, bounded by two concentric circles of radii r_1 = 9 mm and r_2 = 13 mm. The rotation speed of 1,300 rpm was used in all runs, which created an average shear stress of 13 Pa in the active (annular) region on the membrane surface. The micrograph of the membrane surface in Figure 1b shows a square pore array with a pitch of 200 μm.

Preparation of RAPA-PCL NPs. The cell was filled with 60 mL of the aqueous phase and the stirrer speed was adjusted at 1,300 rpm. The organic phase was introduced at 0.65 mL min^{-1} using a Cole-Parmer model 230 VAC syringe pump to achieve a transmembrane flux of 140 L m^{-2} h^{-1}. Each experiment was run until 6 mL of the organic phase was injected and an aqueous-to-organic volumetric ratio reached 10, which took 9.2 min. The aqueous phase turned cloudy as soon as the organic phase was brought in contact with the aqueous phase, due to the formation of NPs that caused ambient light scattering as a result of different refractive index of water (1.33) and PCL (1.47). Once the desired amount of organic phase had passed through the membrane, both the pump and stirrer were switched off and the nanosuspension was collected for further analyses. Figure 1b depicts a solvent displacement mechanism of NPs formation, characterised by a rapid exchange of water and organic solvent between the two phases. The organic solvent was evaporated from the nanosuspension in a vacuum oven (Fistreem International Ltd, Loughborough, UK) at room temperature under an absolute pressure below 10 Torr until the smell of organic solvent had completely disappeared (~30 min). Every experiment was carried out at least three times.

After each run, the membrane was rinsed with Mili-Q water and sonicated in acetone for 30 min using a Fisher Scientific, Model FB 15046, ultrasonic bath. The membrane was then rinsed with Milli-Q water and washed with fresh Milli-Q water in the ultrasonic bath for 5 min.

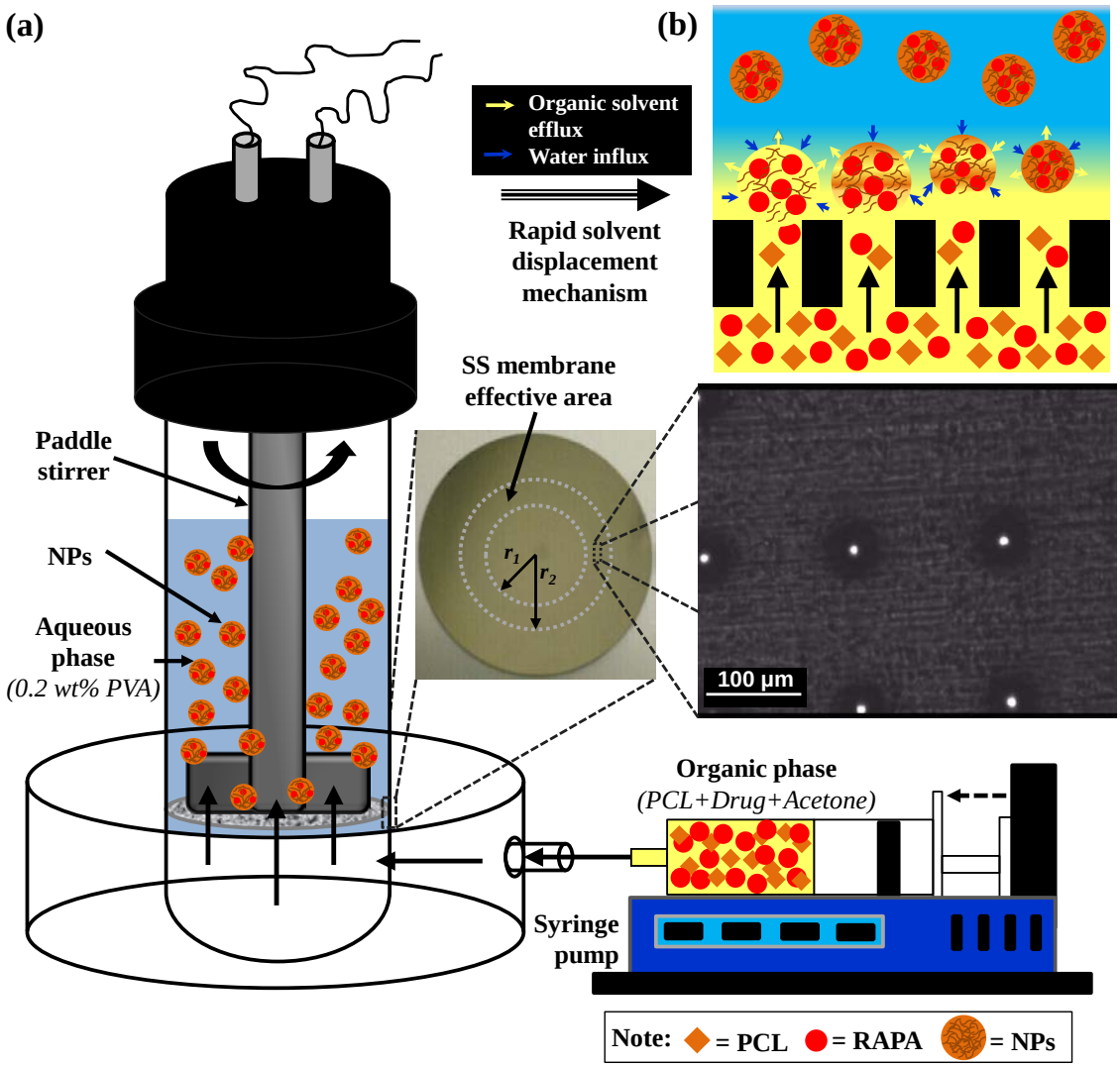

Figure 1. (a) A schematic diagram of the dispersion cell device with a micrograph of a 10-µm ringed SS membrane; (b) Permeation of the organic phase through the membrane and rapid solvent displacement at the interface between the finely dispersed organic phase droplets and the aqueous phase, leading to the precipitation of PCL and formation of RAPA-PCL NPs.

Determination of encapsulation efficiency and drug loading. After complete solvent evaporation, the nanosuspension was ultracentrifuged (Heraeus Labofuge 400R centrifuge, Thermo Scientific) at 15,000 rpm (23,000 g) for 1 h. The supernatant containing the dissolved free drug was separated from the sediment and analysed by an established Reverse phase High Performance Liquid Chromatographic (RP-HPLC) method. Briefly, 20 µL of each sample was injected in a Symmetry® C-8 column (4.6 × 50 mm, 3.5 µm, Waters, UK) eluted with methanol/1 % (v/v) acetic acid in deionised water (75/25 v %) at a flowrate of 1.0 mL min^{-1}. A LC-10Avp Shimadzu UV-VIS detector was used to detect RAPA at 278 nm and ambient temperature. The concentration of RAPA in the sample was determined from a calibration curve constructed using standard RAPA solutions prepared in acetonitrile. The drug entrapment efficiency (E.E.) was calculated from eq. (1):

$$\%E.E. = [1-(M_R/M_T)] \times 100\% \quad (1)$$

where M_R is the mass of RAPA in the supernatant and M_T is the total mass of RAPA in the sample.[11,14,16] The drug loading (D.L.) was calculated from:

$$\%D.L. = [(M_T - M_R)/M_{NP})] \times 100\% \quad (2)$$

where M_{NP} is the total mass of NPs in the sample.[35,36] The analyses were carried out in triplicates and the results were expressed as the mean ± SD (n = 3).

Characterisation of the prepared NPs. *Particle size analysis.* The NPs size distribution was determined by Dynamic Light Scattering (DLS) using a DelsaTM Nano HC Particle Analyser (Beckman Coulter, High Wycombe, UK), which measures the fluctuations in scattered light intensity as a function of time.[37] Smaller NPs move faster than larger NPs and therefore, the timescale of intensity fluctuations is shorter for smaller NPs. A solvent-free nanosuspension was transferred into a 4 mL disposable cuvette which was then placed into the instrument. The data acquisition time was 120 s for each run and the measurements were repeated thrice at 25 °C and 1650 scattering angle using CONTIN and Cumulant fitting algorithms. The Cumulant algorithm provides the z-average size, which is the harmonic intensity averaged particle diameter and the polydispersity index (PDI), which is a dimensionless measure of the broadness of the size distribution. The CONTIN algorithm was developed by Provencher et al. and imparts average peak diameter values from intensity size distribution.[38]

Transmission Electron Microscopy (TEM). RAPA-PCL NPs, blank NPs and RAPA nanocrystals were observed by JEOL JEM-2000FX analytical TEM operated at an accelerating voltage of 200 kV and fitted with an Oxford Instruments Inca EDX system. A drop of the free organic solvent sample was deposited onto a carbon-coated copper mesh and left to dry before observation. The mesh was coated by dipping it into a suspension of carbon particles in deionised water.

Differential Scanning Calorimetry (DSC). The interactions between different ingredients in the synthesised NPs were estimated using a TA Instruments Model Q10 calorimeter. The samples (pure RAPA, pure PCL, blank PCL NPs, a physical mixture of blank PCL NPs and RAPA, and RAPA-PCL NPs), weighting 5 mg each, were hermetically sealed in separate aluminium pans. The sample pans were then heated from 30 to 220 °C at a rate of 10 °C min^{-1} and the DSC profiles were compared with an empty pan. Dry nitrogen at 10 mL min^{-1} was used as the purge gas. RAPA-PCL NPs and blank PCL NPs were prepared by freeze-drying the sediment after centrifugation in a freeze dryer (Edwards, type EF4 Modulyo). Triple runs were carried out on each sample to check reproducibility.

X-Ray Diffractometry (XRD). XRD patterns of pure RAPA, pure PCL, blank PLC NPs, a physical mixture of blank PCL NPs and RAPA, and RAPA-PCL NPs were recorded using a Bruker D8 diffractometer by exposing samples to CuKa radiation (40 kV, 20 mA) over the 2θ range from 5° to 50°, with a step size of 0.02°, an acquisition time per step of 5 s and a scanning speed of 0.5° min^{-1}. The samples were prepared by injection moulding under nitrogen at 100 °C and transferred at ambient temperature to a circular mould with a diameter of 20 mm and a thickness of 1 mm. Triple runs were carried out on each sample to check reproducibility.

Attenuated Total Reflection-Fourier Transform Infrared (ATR-FTIR) Spectroscopy. ATR-FTIR was performed to detect the presence of RAPA in the polymer matrix and investigate possible interactions between RAPA and the host polymer. The IR spectra were recorded in the range of 4000–400 cm^{-1} using a Thermo Scientific Nicolet iS50 ATR spectrometer with a monolithic diamond crystal. 2–3 mg of the pulverised sample was placed onto the Universal diamond ATR top-plate and the spectrum was acquired within 32 s. Triple runs were carried out on each sample to check reproducibility.

In vitro drug release studies. In vitro dissolution testing of poorly water-soluble drug formulations pose significant problems, because the extent of drug release is often too low and the rate of release is too slow for a practical test. In this study, the enhancement of the aqueous solubility of RAPA has been achieved by facilitated hydrotropy.[39] Hydrotropy is a collective molecular phenomenon associated with an increase in the aqueous solubility of a poorly water-soluble compound by addition of a relatively large amount of a second solute, i.e. a hydrotrope.[40] The hydrotropic activity of a hydrotrope can be enhanced by adding water miscible cosolvent(s), which is known as the facilitated hydrotropy. In this work, N,N-diethylnicotinamide (DENA) was used as a hydrotropic agent and its solubilising effect was enhanced by adding ethanol and Tween 20 (polysorbate 20) in the dissolution medium. The RAPA release profiles have been assessed using 0.3 wt% RAPA-PCL NPs and the dissolution/release medium was prepared by mixing 10 vol% of pure (200 proof) ethanol, 10 vol% of 20 % Tween 20, 25.9 vol% of aqueous DENA solution (5.8 M or 3 M), 44.1 vol% of Milli-Q® water, and 10 vol% of 10x phosphate buffered saline (PBS). A known amount of lyophilised sample (5 mg) was placed in a centrifuge tube and dissolved in 5 mL of the dissolution medium. The tube was then incubated in a shaking bath at 50 rpm and 37 °C to mimic the human blood stream conditions.[41] At predetermined time intervals, the test tube was taken out of the shaker and centrifuged at 15,000 rpm for 30 min at −4 °C. The supernatant was removed and the amount of RAPA released was quantified by RP-HPLC method as described above. The volume sampled was replenished with fresh medium to keep the total volume of the release medium constant. All experiments were run in triplicate and the results were expressed as a mean value ± S.D.

Results and Discussion

Effect of organic solvent and organic/aqueous ratio. The selection of suitable organic solvent is a crucial initial step that should be taken in the design of the nanoprecipitation process. The chosen solvent should be able to dissolve the drug and polymer and should be miscible with water. In this series of experiments, blank PCL NPs were prepared using two different organic solvents,

THF and acetone, and in each case five aqueous-to organic volumetric ratios have been tested. The z-average mean decreased with increasing the aqueous-to-organic volumetric ratio, as shown in Figure 2. The same trend was observed for itraconazole and ZnO NPs prepared via SPG membrane,[42,43] and liposomes and micelles produced using nickel membrane.[27,44,45]. The size of NPs formed by anti-solvent precipitation is a result of the relative rates of nucleation, particle growth, and agglomeration. The faster removal of solvent at higher V_{aq}/V_{or} values led to higher supersaturation levels, which promoted nucleation over particle growth and resulted in smaller NPs. In addition, agglomerates are less likely to form in more diluted suspensions, because they can only form when NPs collide with each other and the collision frequency of NPs is proportional to the second power of their number density.

The Z-average mean was consistently smaller when the NPs were formed using THF as compared to acetone. The solvent-PCL distance in the "$2\delta_d–\delta_p–\delta_h$" solubility space is equal to 1.08 and 6.53 for THF and acetone, respectively,[20] which means that PCL is more soluble in THF than acetone. Thus, compared to acetone, THF must be diluted with water to a greater extent for PCL to begin to precipitate, which means that the growing NPs are less likely to agglomerate. The same type of behaviour with smaller NPs formed using THF than acetone was observed for fluconazole-loaded polymeric micelles produced by membrane and microfluidic nanoprecipitation.[46] Although PCL NPs are smaller in the presence of THF, in subsequent experiments RAPA-PCL NPs will be formed using acetone, because RAPA is sparingly soluble in THF and the difference in size between the NPs formed using acetone and THF is only 3-8 %. To obtain the smallest possible NPs size, the ratio V_{aq}/V_{or} will be kept at 10.

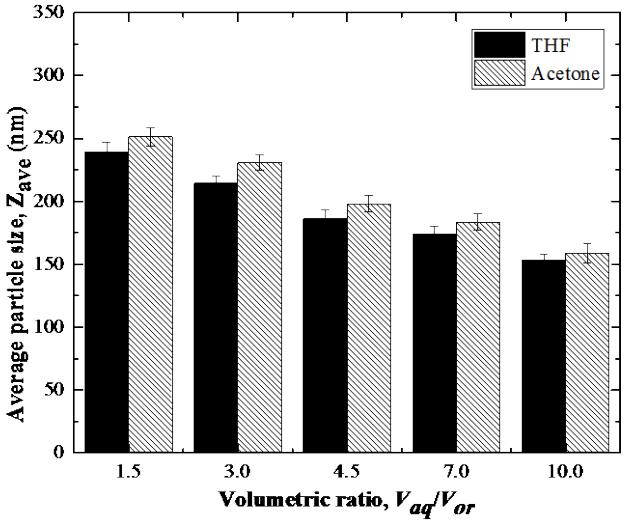

Figure 2. The Z-average size of blank PCL NPs produced using two different organic solvents (THF and acetone) at different aqueous/organic phase volumetric ratios.

Drug encapsulation efficiency and drug loading. RAPA-PCL NPs were larger than blank PCL NPs formed under the same conditions and their size increased from 189 ± 4 nm to 218 ± 5 nm with increasing the drug/excipient ratio in the organic phase from 0.1 to 0.5 (Table 1). A size uniformity of the NPs deteriorated with an increase in the drug/excipient ratio, as revealed by an increase in PDI from 0.006 to 0.073. It is worth mentioning that PDI values smaller than 0.05 are rarely seen other than with highly monodispersed standards. The encapsulation efficiency of RAPA was ≥ 98.8 %, due to very low aqueous solubility of RAPA and strong hydrophobic interactions between RAPA and PCL. Based on RAPA solubility in water of 0.0026 mg·mL^{-1} at 25 °C, the maximum amount of RAPA that could be dissolved was 0.156 mg per batch and the amount of RAPA added in the organic phase was 3.6–18 mg per batch, which means that the maximum loss of RAPA due to its dissolution was 0.9–4.3 %. However, the RAPA solubility in the aqueous phase was greater than 0.0026 mg·mL-1 due to the presence of acetone diffused from the organic phase. The RAPA loading in the NPs increased from 9.0 wt% to 33.0 wt% when a RAPA/PCL mass ratio in the organic phase increased from 0.1 to 0.5. The maximum theoretical drug loading corresponding to these drug-excipient ratios was 9.1 and 33.3 %, which nearly perfectly matches experimental values and proves that almost all RAPA was entrapped in the NPs. The similar trends were observed by Zhang et al. who reported an increase in the particle size (170 to 180 nm), encapsulation efficiency (84.1 to 99.7 %) and drug loading (5.03 to 14.91 %) when a RAPA/polymer ratio in the organic phase increased from 5 to 15 %.[13]

Table 1: The effect of RAPA-to-PCL mass ratio in the organic phase on the average particle size, Z_{ave}, drug encapsulation efficiency, E.E., and drug loading, D.L.. The organic phase was prepared by dissolving RAPA and 6 g L^{-1} of PCL in acetone and V_{aq}/V_{or} = 10.

RAPA/PCL mass ratio in organic phase	Volumetric ratio, V_{aq}/V_{or} = 10			
	E.E. (%)	D.L. (%)	Average size of NPs, Z_{ave} (nm)	Polydispersity index (PDI)
0.1	98.79	8.98	189 ± 4	0.006 ± 0.025
0.2	98.80	16.47	195 ± 4	0.040 ± 0.031
0.3	98.92	22.83	198 ± 7	0.030 ± 0.024
0.4	98.91	28.26	204 ± 1	0.066 ± 0.035
0.5	98.93	32.98	218 ± 5	0.073 ± 0.023

* Note: Each analysis was repeated three times (n = 3) and the average particle sizes were determined. The error bars are standard deviations.

Characterisation of the NPs. *TEM analysis of the NPs.* TEM micrographs shown in Figure 3 revealed that blank PCL and RAPA-PCL NPs were uniform discrete nanospheres. RAPA-PCL NPs were larger than blank PCL NPs, probably because RAPA was embedded or solubilised in the PCL matrix of the NPs, which is consistent with the results in Table 1. RAPA nanocrystals (NCs) were of irregular shape and bigger than RAPA-PCL NPs due to aggregation of RAPA nanocrystallites in the absence of PCL host. No free crystals were found in the sample of RAPA-PCL NPs.

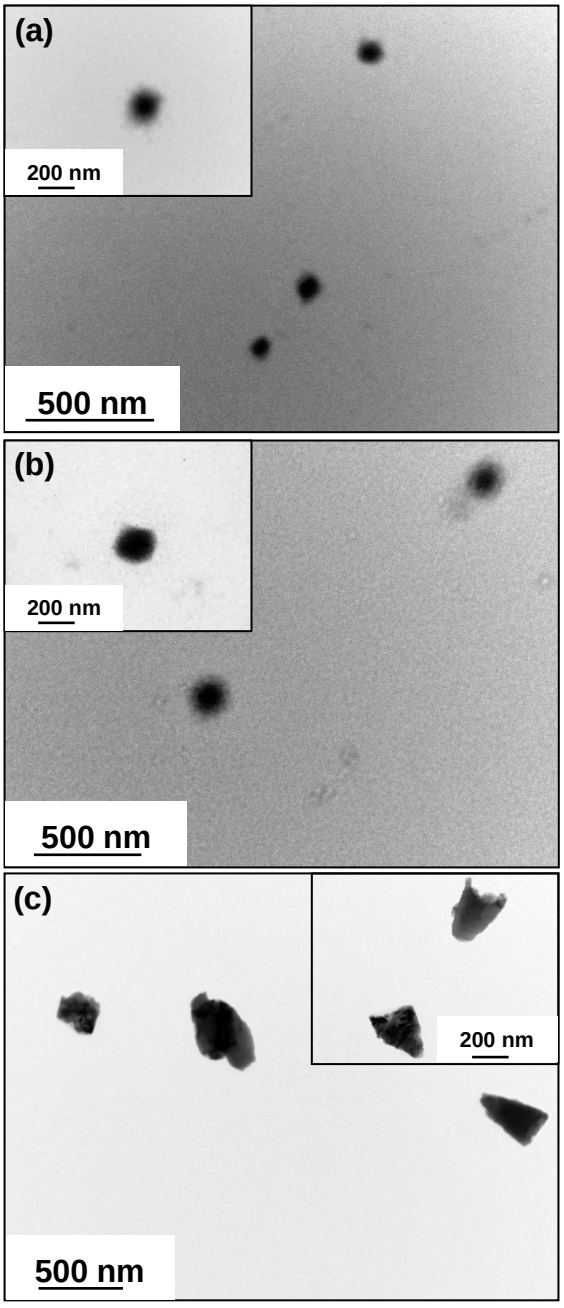

Figure 3. TEM images of the NPs prepared under identical experimental conditions: (a) blank PCL NPs; (b) RAPA-PCL NPs; and (c) pure RAPA nanocrystals without PCL host. RAPA-PCL NPs were prepared using the drug-to-excipient mass ratio in the organic phase of 0.4.

TEM images in Figure 3 are well correlated with the intensity size distributions of the NPs shown in Figure 4. Blank PCL and RAPA-PCL NPs were very uniform in size and smaller than RAPA NCs due to the suppression of crystal growth by the host polymer. RAPA NCs had a broader size distribution due to stochastic nature of the agglomeration process and the average particle size was larger than 500 nm. These results indicate the importance of drug entrapment within a polymer host for obtaining the NPs smaller than 250 nm and the capability of ringed stainless steel membrane with laser-drilled pores to generate nearly monodispersed NPs.

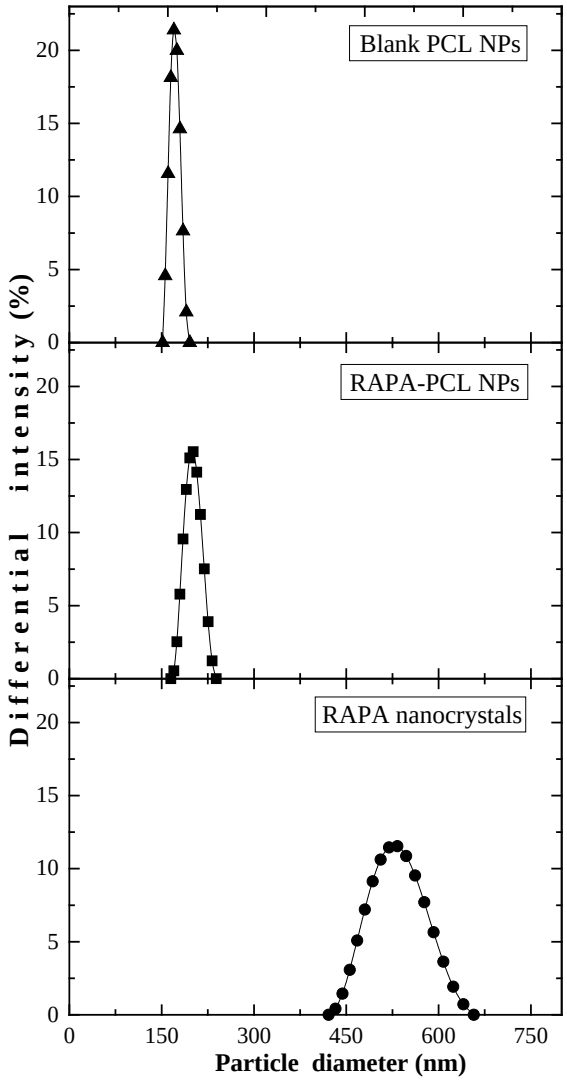

Figure 4. The intensity size distributions of blank PCL NPs, RAPA-PCL NPs, and RAPA nanocrystals produced under identical experimental conditions (V_{aq}/V_{or} = 10, transmem-

brane flux = 140 $Lm^{-2}h^{-1}$, stirrer speed = 1300 rpm). The formulations are indicated in section 2.1.

XRD analysis. XRD analysis was used to determine the degree of PCL crystallinity in the NPs, i.e. if the encapsulated drug is mainly in crystalline form or molecularly dispersed. It is important because different physical states of the drug within polymer network exhibit different storage stability, solubility, dissolution rate, and bioavailability, which may significantly affect therapeutic effects of the drug. As can be seen in Figure 5a, the XRD pattern 1 of pure crystalline RAPA shows a multitudes of high-intensity peaks at 7.2°, 9.9°, 10.3°, 11.1°, 12.5°, 14.5°, 15.3°, 15.5°, 16.2°, 20.0°, 20.4°, 21.8° and 23.5°. The diffraction pattern 2 of pure PCL shows two peaks at 2θ = 21.4° and 23.8°, corresponding to the (110) and (200) crystallographic planes of semi-crystalline PCL. Similar XRD results for pure RAPA and PCL were obtained by Kim et al.[8] and Yeo et al.[47], respectively. In the XRD pattern 3 of blank PCL NPs, the two characteristic peaks of PCL were shifted leftward and were less intense than in the XRD spectrum of pure PCL. The polymer crystallinity was reduced from 68.9 % in the raw PCL powder to 67.1 % in the NPs, due to rapid polymer precipitation and a lack of time for the polymer chains to arrange themselves in an ordered manner before solidification.[48]

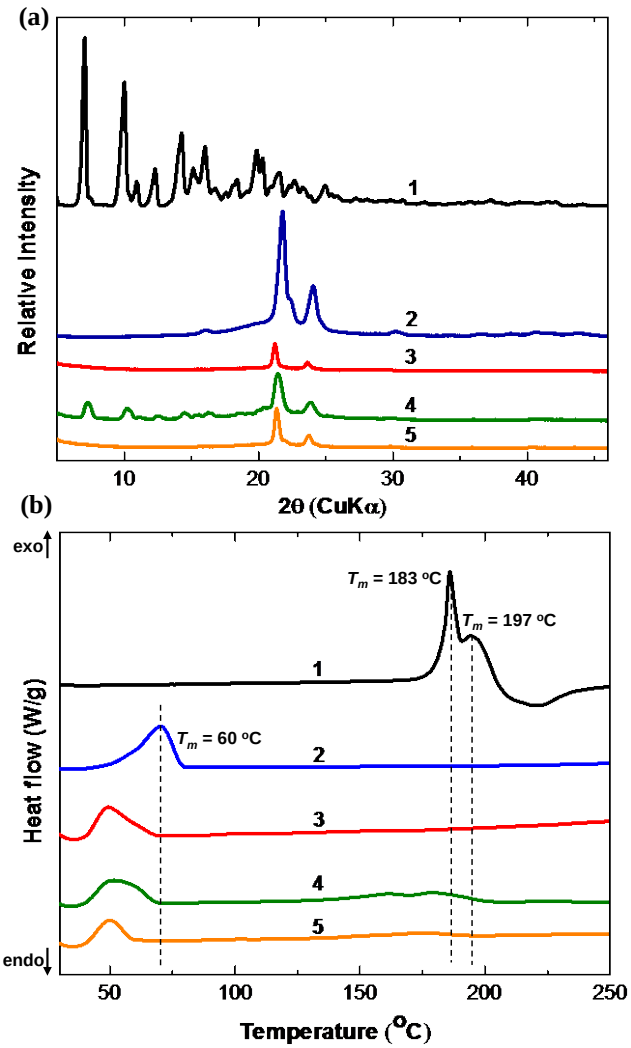

Figure 5. (a) X-ray diffractograms; and (b) DSC thermograms of: 1- pure RAPA; 2- pure PCL; 3-blank PCL NPs; 4- physical mixture of blank PCL NPs and RAPA; and 5-RAPA-PCL NPs.

In the XRD pattern of the physical mixture of blank PCL NPs and pure RAPA, specific peaks of both blank PCL NPs and pure RAPA were observed, suggesting that RAPA was in the crystalline state and did not undergo molecular interactions with blank PCL NPs. In the spectrum 5 of RAPA-PCL NPs, only the PCL peaks at 21.4° and 23.8° were detected, while the characteristic peaks of RAPA disappeared. It indicates that the encapsulated drug was either present in the form of a molecular dispersion in the polymer, i.e. the drug and polymer were homogeneously mixed at the molecular level, or RAPA was present in the form of amorphous domains dispersed in the polymer matrix.[49] Compared to the crystalline state, amorphous drug exhibits greater dissolution rate and greater bioavailability, but also greater chemical reactivity and tendency to revert back to energetically favoured crystalline state. The degree of crystallinity was reduced

from 78.9 % for pure RAPA sample to 71.3 % for the physical mixture of pure RAPA and blank PCL NPs to 63.7 % for RAPA-PCL NPs.

DSC analysis. DSC is a thermodynamic tool used in the pharmacology to measure phase transitions in materials as a function of time and temperature as well as to quantify an amorphous or crystalline phase in NPs and possible interactions between the drug and excipient.[50] The DSC profiles of pure RAPA, pure PCL, blank PCL NPs, mixture of pure RAPA and blank PCL NPs, and RAPA-PCL NPs are shown in Figure 5b. Pure crystalline RAPA exhibited two endothermic peaks at 183 °C and 197 °C, corresponding to the melting points of two different crystalline forms of the drug.[51] Pure PCL polymer exhibited an endothermic peak at 60 °C, corresponding to its melting point.[52]

An endothermic peak in blank PCL NPs was shifted to ~52 °C and more diffuse, revealing the reduced crystallinity of PCL after precipitation. Two endothermic peaks corresponding to the melting points of PCL and RAPA were detected in the physical mixture of pure RAPA and blank PCL NPs. A shallow RAPA peak between 180 and 200 °C can be attributed to the low proportion of the drug in the mixture. A PCL peak of RAPA-PCL NPs occurred at ~50 °C indicating that the polymer chains were more disordered in the presence of RAPA in the polymer matrix than in blank PCL NPs. The absence of RAPA peak in RAPA-PCL NPs confirmed our previous assumption that the drug did not form crystalline domains in the polymer. Similar observations were reported by Zhang et al.[13] and Kim et al. [8].

ATR-FTIR spectroscopy. FTIR analysis was used to investigate chemical integrity of RAPA and PCL during the nanoprecipitation process.[9] The FTIR spectra of different samples are shown in Figure 6. Characteristic bands in pure RAPA appeared at 3418 cm^{-1}, due to O–H stretching vibrations, at 2875 and 2932 cm^{-1} due to C–H stretching vibrations, and at 1718 cm^{-1} due to C=O stretching. Besides, the peak at 1377 cm^{-1} was due to ≡CH bending and the peaks at 1635 cm^{-1} and 995 cm^{-1} could be assigned to the existence of double bonds: the peak at 1635 cm^{-1} was due to C=C stretching and the peak at 995 cm^{-1} was due to =C–H bending.

The two peaks in the pure PCL spectrum at 2942 cm^{-1} and 2867 cm^{-1} were due to C–H stretching in the hydrocarbon chains of PCL and the strongest peak at ~1720 cm^{-1} was due to the C=O stretching in the ester groups. The strong peak at 1181 cm^{-1} could be assigned to C–O stretching of ester linkages.[53] Besides, the asymmetric bending vibrations of methyl groups and the bending vibration of methylene group are located in the 1460 cm^{-1} region of pure PCL spectrum. The peaks at 3418 cm^{-1} and 1635 cm^{-1} found in the pure RAPA spectrum are missing in the pure PCL spectrum, due to absence of O–H and C=C bonds, respectively.

No change in the position of various bands was found in the spectrum of blank PCL NPs compared with that of pure PCL, which means that FTIR could not prove any change in the chemical structure of PCL as a result of dissolution and precipitation. New small peaks at 995 cm^{-1} and 1635 cm^{-1} detected in the spectrum of the mixture of pure RAPA and blank PCL NPs were inherited from pure RAPA. The peak at 1635 cm^{-1} due to C=C stretching was visible in the spectrum of RAPA-PCL NPs, but it was tiny and unshifted. This indicates that RAPA was encapsulated within the NPs matrices, but has not strongly interacted with PCL.

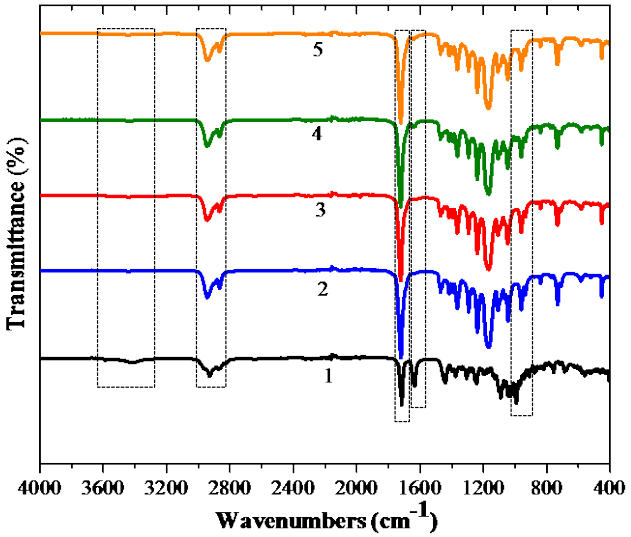

Figure 6. ATR-FTIR spectra of: 1- pure RAPA; 2- pure PCL; 3- blank PCL NPs; 4- physical mixture of RAPA and blank PCL NPs; and 5- RAPA-PCL NPs.

In vitro release of RAPA from RAPA-PCL NPs. A fast and complete release of encapsulated drug from NPs after oral administration is an important desirable feature of pharmaceutical formulations. The amount of RAPA released from RAPA-PCL NPs and RAPA NCs is shown in Figure 7 with zero-time corresponding to the start of the incubation period. A complete dissolution of RAPA from NCs was achieved after 2.5 h using the dissolution mixture containing 0.78 M DENA, 10 vol% ethanol, and 2 vol% Tween 20 in PBS. After 18 h, a total of 91.3 % and 93.8 % of the drug were released from RAPA-PCL NPs in 0.78 M and 1.5 M DENA solution, respectively. The remaining amount of RAPA (6.2–8.7 %) was firmly bound to the polymer chains due to strong drug-polymer interactions and could only be released by complete degradation of the polymer matrix. A burst release of more than 80 % of RAPA was observed over the first 1 hour. The fastest release was observed from RAPA NCs due to the absence of PCL host. The Peppas empirical model[54] was the most appropriate model to fit the release data for small values of time: $M_R/M_\infty = kt^n$, where M_R/M_∞ is the fraction of RAPA released at time t. The release exponent n was

found to range between 0.83 and 0.90, which means that the drug was released by non-Fickian diffusion.

The higher amount of RAPA was released in the dissolution medium containing higher concentration of DENA. The previous research[55] confirmed that DENA is as an efficient hydrotropic agent for accelerated release of paclitaxel, another poorly water-soluble drug, from biodegradable polymer matrices. The potential mechanisms of hydrotropic action of DENA are stacking complexation, chaotropic activity, and self-association.[56] Stacking complexation between the planar aromatic rings of DENA and RAPA occurs due to tendency of the system to minimise the exposure of hydrophobic molecular regions to water. DENA also acts as a chaotropic agent disrupting the hydrogen bonds between water molecules, which results in the higher solubility of nonpolar solutes. Finally, DENA can self-assemble into micelles, followed by the incorporation of RAPA into their hydrophobic cores,[56] which increases the solubility of RAPA. No drug release from RAPA-PCL NPs was detected after 18 h of incubation in pure water, due to poor aqueous solubility of RAPA (2.6 μmL-1 at 25 °C).[39]

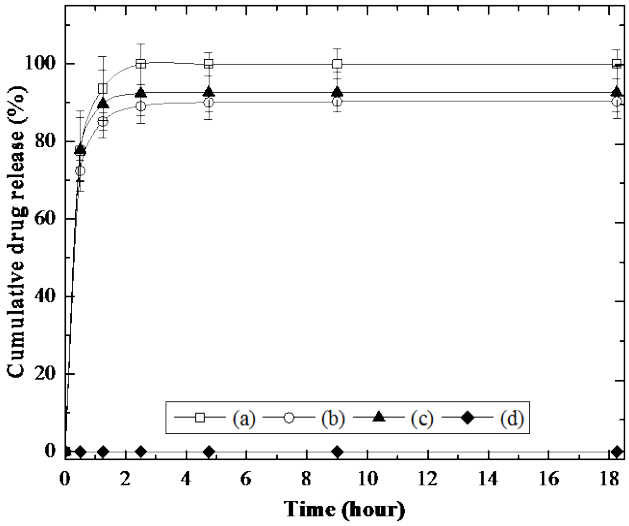

Figure 7. The release profile of RAPA from: (a) RAPA NCs in 0.78 M DENA solution; (b) RAPA-PCL NPs in 0.78 M DENA solution; (c) RAPA-PCL NPs in 1.5 M DENA solution; and (d) RAPA-PCL NPs in water. The dissolution medium is an aqueous solution containing 0.78 or 1.5 M DENA, 10 vol% of ethanol, 2 vol% of Tween 20, and 1X PBS. The error bars represent the standard deviations of three repeated measurements (n = 3).

Conclusions

Polycaprolactone (PCL) NPs loaded with the immunosuppressive drug rapamycin (RAPA) have been facilely prepared by antisolvent precipitation using a ringed stainless steel membrane with laser drilled pores. Due to optimum position of the pores localised in the region of maximum shear, nearly monodispersed particles have been obtained with a polydispersity index (PDI) of 0.006–0.073. The particle size increased with increasing the RAPA content in the polymer network and the drug encapsulation efficiency was above 98.8% in all samples. Drug-loaded PCL NPs were significantly smaller and more uniform than RAPA nanocrystals prepared under the same conditions but without PCL host, revealing the important role of PCL in inhibiting particle growth and agglomeration during nanoprecipitation.

The encapsulation of RAPA in the PCL matrix was confirmed by UV-Vis spectroscopy, XRD, DSC, and ATR-FTIR. The disappearance of characteristic sharp peaks of crystalline RAPA in the XRD pattern of RAPA-PCL NPs revealed that the drug was molecularly dispersed in the polymer matrix or the drug and polymer were present in individual amorphous domains. When RAPA-PCL NPs were stored in pure water at room temperature, the release of RAPA could not be detected due to negligible aqueous solubility of RAPA. However, drug-loaded NPs released more than 91 % of their drug cargo after 2.5 h of incubation in the dissolution medium composed of the mixture of the hydrotropic agent N,N-diethylnicotinamide, ethanol, and a non-ionic surfactant, Tween 20 in phosphate buffered saline. The dissolution of RAPA was slower when the drug was embedded in the PCL matrix of the NPs than present in the form of pure RAPA nanocrystals. The prepared NPs can be used for a prolonged drug release in anti-cancer and anti-restenotic therapies. Our future work will be focused on the in-vivo drug release studies in order to simulate the actual body conditions. The production of uniform drug nanocrystals will be also optimized.

AUTHOR INFORMATION

Corresponding Author

* Email: R.Othman@lboro.ac.uk (Rahimah Othman) or G.Vladisavljevic@lboro.ac.uk (Goran T. Vladisavljević).

Author Contributions

The manuscript was written through contributions of all authors. All authors have given approval to the final version of the manuscript.

ACKNOWLEDGMENT

The authors acknowledge the financial support for this work through the Ministry of Higher Education Malaysia and the technical assistance by Dr Zhaoxia Zhou and Dr Keith Yendall from the Department of Materials at Loughborough University for TEM and XRD analyses. The authors also acknowledge the financial support provided by the EPSRC grant EP/HO29923/1 and the European Research Council grant [280106-CrySys].

ABBREVIATIONS

(RAPA-PCL NPs), rapamycin loaded polycaprolactone nanoparticles; (UV-Vis), ultraviolet–visible; (TEM), transmission electron microscopy; (XRD), x-ray diffractometry; (DSC), differential scanning calorimetry; (ATR-FTIR), attenuated

total reflection-Fourier transform infrared; (DENA), N,N-diethylnicotinamide.

REFERENCES

(1) Barratt, G. M. Therapeutic Applications of Colloidal Drug Carriers. *Pharm. Sci. Technolo. Today* **2000**, *3* (5), 163–171.

(2) Torchilin, V. Multifunctional and stimuli-sensitive pharmaceutical nanocarriers, *Eur. J. Pharm. Biopharm* ***2009***, 71 (2), 431–444.

(3) Caban, S.; Aytekin, E.; Sahin, A.; Capan, Y. Nanosystems for Drug Delivery. *OA Drug Des. Deliv.* **2014**, *2* (1), 1–7.

(4) Kumari, A.; Yadav, S. K.; Yadav, S. C. Biodegradable Polymeric Nanoparticles Based Drug Delivery Systems. *Colloids Surf. B. Biointerfaces* **2010**, *75* (1), 1–18.

(5) Fessi, H.; Devissaguet, J.P.; Puisieux, F.; Thies, C. Process for the preparation of dispersible colloidal systems of a substance in the form of nanoparticles, *U.S. Patent* **1992**, 5 118 528, Jun 2.

(6) Fessi, H.; Puisieux, F. Nanocapsule formation by interfacial polymer deposition following solvent displacement, *Int. J. Pharm.* **1989**, 55 (1) R1–R4.

(7) Jain, R.A. The manufacturing techniques of various drug loaded biodegradable poly(lactide-co-glycolide) (PLGA) devices, *Biomaterials* **2000**, 21 (23) 2475–2490.

(8) Kim, M. S.; Kim, J. S.; Park, H. J.; Cho, W. K.; Cha, K. H.; Hwang, S. J. Enhanced Bioavailability of Sirolimus via Preparation of Solid Dispersion Nanoparticles Using a Supercritical Antisolvent Process. *Int. J. Nanomedicine* **2011**, *6*, 2997–3009.

(9) Acharya, S.; Dilnawaz, F.; Sahoo, S. K. Targeted Epidermal Growth Factor Receptor Nanoparticle Bioconjugates for Breast Cancer Therapy. *Biomaterials* **2009**, *30* (29), 5737–5750.

(10) Luderer, F.; Löbler, M.; Rohm, H. W.; Gocke, C.; Kunna, K.; Köck, K.; Kroemer, H. K.; Weitschies, W.; Schmitz, K.-P.; Sternberg, K. Biodegradable Sirolimus-Loaded Poly(lactide) Nanoparticles as Drug Delivery System for the Prevention of in-Stent Restenosis in Coronary Stent Application. *J. Biomater. Appl.* **2011**, *25* (8), 851–875.

(11) Zou, J.; Zhang, X.; Yang, H.; Zhu, Y.; Ma, H.; Wang, S. Rapamycin-Loaded Nanoparticles for Inhibition of Neointimal Hyperplasia in Experimental Vein Grafts. *Ann. Vasc. Surg.* **2011**, *25* (4), 538–546.

(12) Shi, X.; Chen, G.; Guo, L. W.; Si, Y.; Zhu, M.; Pilla, S.; Liu, B.; Gong, S.; Kent, K. C. Periadventitial Application of Rapamycin-Loaded Nanoparticles Produces Sustained Inhibition of Vascular Restenosis. *PLoS One* **2014**, *9* (2), 1–12.

(13) Zhang, Z.; Xu, L.; Chen, H.; Li, X. Rapamycin-Loaded Poly(ε-Caprolactone)-Poly(ethylene Glycol)-Poly(ε-Caprolactone) Nanoparticles: Preparation, Characterization and Potential Application in Corneal Transplantation. *J. Pharm. Pharmacol.* **2013**, *66* (4), 557–563.

(14) Chen, Y. C.; Lo, C. L.; Lin, Y. F.; Hsiue, G. H. Rapamycin Encapsulated in Dual-Responsive Micelles for Cancer Therapy. *Biomaterials* **2013**, *34* (4), 1115–1127.

(15) Zweers, M. L. T.; Engbers, G. H. M.; Grijpma, D. W.; Feijen, J. Release of Anti-Restenosis Drugs from Poly(ethylene Oxide)-Poly(dl-Lactic-Co-Glycolic Acid) Nanoparticles. *J. Control. Release* **2006**, *114* (3), 317–324.

(16) Yuan, X. B.; Yuan, Y. B.; Jiang, W.; Liu, J.; Tian, E. J.; Shun, H. M.; Huang, D. H.; Yuan, X. Y.; Li, H.; Sheng, J. Preparation of Rapamycin-Loaded chitosan/PLA Nanoparticles for Immunosuppression in Corneal Transplantation. *Int. J. Pharm.* **2008**, *349* (1-2), 241–248.

(17) Bae, Y. H.; Park, K. Targeted Drug Delivery to Tumors: Myths, Reality and Possibility. *J. Control. Release* **2011**, *153* (3), 198–205.

(18) Chen, G. G.; Luo, G. S.; Xu, J. H.; Wang, J. D. Membrane Dispersion Precipitation Method to Prepare Nanopartials. *Powder Technol.* **2004**, *139* (2), 180–185.

(19) Charcosset, C.; Fessi, H. Preparation of Nanoparticles with a Membrane Contactor. *J. Memb. Sci.* **2005**, *266* (1-2), 115–120.

(20) Vladisavljević, G. T.; Laouini, A.; Charcosset, C.; Fessi, H.; Bandulasena, H. C. H.; Holdich, R. G. Production of Liposomes Using Microengineered Membrane and Co-Flow Microfluidic Device. *Colloids Surf. A* **2014**, 458 (1) 168–177.

(21) Othman, R.; Vladisavljević, G. T.; Hemaka Bandulasena, H. C.; Nagy, Z. K. Production of Polymeric Nanoparticles by Micromixing in a Co-Flow Microfluidic Glass Capillary Device. *Chem. Eng. J.* **2015**, *280*, 316–329.

(22) Limayem B. I.; Charcosset, C.; Sfar, S.; Fessi, H. Preparation and Characterization of Spironolactone-Loaded Nanocapsules for Paediatric Use. *Int. J. Pharm.* **2006**, *325* (1-2), 124–131.

(23) Laouini, A; Jaafar-Maalej, C.; Sfar, S.; Charcosset, C.; Fessi, H. Liposome Preparation Using a Hollow Fiber Membrane Contactor--Application to Spironolactone Encapsulation. *Int. J. Pharm.* **2011**, *415* (1-2), 53–61.

(24) Jaafar-Maalej, C.; Charcosset, C.; Fessi, H. A New Method for Liposome Preparation Using a Membrane Contactor. *J. Liposome Res.* **2011**, *21* (3), 213–220.

(25) Dragosavac, M. M.; Holdich, R. G.; Vladisavljević, G. T.; Sovilj, M. N. Stirred Cell Membrane Emulsification for Multiple Emulsions Containing Unrefined Pumpkin Seed Oil with Uniform Droplet Size. *J. Memb. Sci.* **2012**, *392-393*, 122–129.

(26) Laouini, A.; Charcosset, C.; Fessi, H.; Holdich, R. G.; Vladisavljević, G. T. Preparation of Liposomes: A Novel Application of Microengineered Membranes - Investigation of the Process Parameters and Application to the Encapsulation of Vitamin E. *RSC Adv.* **2013**, *3* (15), 4985–4994.

(27) Imbrogno, A.; Dragosavac, M. M.; Piacentini, E.; Vladisavljević, G. T.; Holdich, R. G.; Giorno, L. Polycaprolactone Multicore-Matrix Particle for the Simultaneous Encapsulation of Hydrophilic and Hydrophobic Compounds Produced by Membrane Emulsification and Solvent Diffusion Processes. *Colloids Surfaces B Biointerfaces* **2015**, *135*, 116–125.

(28) Warkiani, M. E.; Bhagat, A. A. S.; Khoo, B. L.; Han, J.; Lim, C. T.; Gong, H. Q.; Fane, A. G. Isoporous Micro/nanoengineered Membranes. *ACS Nano* **2013**, *7* (3), 1882–1904.

(28) Holdich, R. G.; Dragosavac, M. M.; Vladisavljević, G. T.; Piacentini, E. Continuous Membrane Emulsification with Pulsed (Oscillatory) Flow. *Ind. Eng. Chem. Res.* **2012**, *52* (1), 507–515.

(29) Holdich, R. G.; Dragosavac, M. M.; Vladisavljević, G. T.; Kosvintsev, S. R. Membrane Emulsification with Oscillating and Stationary Membranes. *Ind. Eng. Chem. Res.* **2010**, *49* (8), 3810–3817.

(30) Silva, P. S.; Dragosavac, M. M.; Vladisavljević, G. T.; Bandulasena H. C. H.; Holdich, R. G. Azimuthally Oscillating Membrane Emulsification for Controlled Droplet Production. *AIChE J.* **2015**, *61* (11), 3607–3615.

(31) Othman, R.; Vladisavljević, G. T.; Shahmohamadi, H.; Nagy, Z. K.; Holdich, R. G. Formation of Size-Tuneable Biodegradable Polymeric Nanoparticles by Solvent Displacement Method Using Micro-Engineered Membranes Fabricated by Laser Drilling and Electroforming. *Chem. Eng. J.* **2016**, *304*, 703–713.

(32) Lemoine, D.; Francois, C.; Kedzierewicz, F.; Preat, V.; Hoffman, M.; Maincent, P. Stability Study of Nanoparticles of Poly(ε-Caprolactone), Poly(D,L-Lactide) and Poly(D,L-Lactide-Co-Glycolide). *Biomaterials* **1996**, *17* (22), 2191–2197.

(33) Woodruff, M. A.; Hutmacher, D. W. The Return of a Forgotten polymer—Polycaprolactone in the 21st Century. *Prog. Polym. Sci.* **2010**, 35 (10), 1217–1256.

(34) Yuan, X. B.; Yuan, Y. B.; Jiang, W.; Liu, J.; Tian, E. J.; Shun, H. M.; Huang, D. H.; Yuan, X. Y.; Li, H.; Sheng, J. Preparation of Rapamycin-Loaded chitosan/PLA Nanoparticles for Immunosuppression in Corneal Transplantation. *Int. J. Pharm.* **2008**, *349* (1-2), 241–248.

(35) Othman, R.; Vladisavljević, G. T.; Thomas, N. L.; Nagy, Z. K. Fabrication of Composite Poly(D,L-Lactide)/montmorillonite Nanoparticles for Controlled Delivery of Acetaminophen by Solvent-Displacement Method Using Glass Capillary Microfluidics. *Colloids Surf. B* **2016**, 141 () 187–195.

(36) Othman, R.; Vladisavljević, G. T.; Nagy, Z. K. Preparation of Biodegradable Polymeric Nanoparticles for Pharmaceutical Applications Using Glass Capillary Microfluidics. *Chem. Eng. Sci.* **2015**, *137*, 119–130.

(37) D.N. Submicron, D. N. User's Manual: Delsa™ Nano Subricon Particle Size and Zeta Potential, Beckman Coulter Ireland Inc., Ireland, **2011**.

(38) Provencher, S. W.; Hendrix, J.; De Maeyer, L.; Paulussen, N. Direct Determination of Molecular Weight Distributions of Polystyrene in Cyclohexane with Photon Correlation Spectroscopy. *J. Chem. Phys.* **1978**, *69* (9), 4273–4276.

(39) Simamora, P.; Alvarez, J. M.; Yalkowsky, S. H. Solubilization of Rapamycin. *Int. J. Pharm.* **2001**, *213* (1-2), 25–29.

(40) Lee, J.; Lee, S. C.; Acharya, G.; Chang, C. J.; Park, K. Hydrotropic Solubilization of Paclitaxel: Analysis of Chemical Structures for Hydrotropic Property. *Pharm. Res.* **2003**, *20* (7), 1022–1030.

(41) Behera, A. K.; Shah, S.; Barik, B. B. Development and Enhancement of Entrapment Efficiency of Isoniazid Loaded Poly- ε -Caprolactone Nanoparticle. **2013**, *5* (4), 43–50.

(42) Seo, J. W.; Kim, K. J.; Kim, S. H.; Hwang, K. M.; Seok, S. H.; Park, E. S. Effect of Process Parameters on Formation and Aggregation of Nanoparticles Prepared with a Shirasu Porous Glass Membrane. **2015**, *63* (10), 792–798.

(43) Huang, C.; Wang, Y.; Luo, G. Preparation of Highly Dispersed and Small-Sized ZnO Nanoparticles in a Membrane Dispersion Microreactor and Their Photocatalytic Degradation. *Ind. Eng. Chem. Res.* **2013**, *52* (16), 5683–5690.

(44) Laouini, A.; Koutroumanis, K. P.; Charcosset, C.; Georgiadou, S.; Fessi, H.; Holdich, R. G.; Vladisavljević, G. T. pH-Sensitive Micelles for Targeted Drug Delivery Prepared Using a Novel Membrane Contactor Method. *ACS Appl. Mater. Interfaces* **2013**, *5* (18), 8939–8947.

(45) Laouini, A.; Charcosset, C.; Fessi, H.; Holdich, R. G.; Vladisavljević, G. T. Preparation of Liposomes: A Novel Application of Microengineered Membranes-From Laboratory Scale to Large Scale. *Colloids Surfaces B Biointerfaces* **2013**, *112*, 272–278.

(46) Lu, Y.; Chowdhury, D.; Vladisavljević, G.; Koutroumanis, K.; Georgiadou, S. Production of Fluconazole-Loaded Polymeric Micelles Using Membrane and Microfluidic Dispersion Devices. *Membranes (Basel).* **2016**, *6* (2), 29.

(47) Yeo, M.; Jung, W.-K.; Kim, G. Fabrication, Characterisation and Biological Activity of Phlorotannin-Conjugated PCL/beta-TCP Composite Scaffolds for Bone Tissue Regeneration. *J. Mater. Chem.* **2012**, *22* (8), 3568–3577.

(48) Izumikawa, S.; Yoshioka, S.; Aso, Y.; Takeda, Y. Preparation of poly(L-Lactide) Microspheres of Different Crystalline Morphology and Effect of Crystalline Morphology on Drug Release Rate. *J. Control. Release* **1991**, *15*, 133–140.

(49) Huang, Y.; Dai, W. G. Fundamental Aspects of Solid Dispersion Technology for Poorly Soluble Drugs. *Acta Pharm. Sin. B* **2014**, *4* (1), 18–25.

(50) Gill, P.; Moghadam, T. T.; Ranjbar, B. Differential Scanning Calorimetry Techniques: Applications in Biology and Nanoscience. *J. Biomol. Tech.* **2010**, *21* (4), 167–193.

(51) Rouf, M. A; Vural, I.; Bilensoy, E.; Hincal, A.; Erol, D. D. Rapamycin-Cyclodextrin Complexation: Improved Solubility and Dissolution Rate. *J. Incl. Phenom. Macrocycl. Chem.* **2011**, *70* (1-2), 167–175.

(52) Guilherme, M. R.; Mauricio, M. R.; Tenório-Neto, E. T.; Kunita, M. H.; Cardozo-Filho, L.; Cellet, T. S. P.; Pereira, G. M.; Muniz, E. C.; Da Rocha, S. R. P.; Rubira, A. F. Polycaprolactone Nanoparticles Containing Encapsulated Progesterone Prepared Using a $scCO_2$ Emulsion Drying Technique. *Mater. Lett.* **2014**, *124*, 197–200.

(53) Liau, C. P.; Bin Ahmad, M.; Shameli, K.; Yunus, W. M. Z. W.; Ibrahim, N. A.; Zainuddin, N.; Then, Y. Y. Preparation and Characterization of Polyhydroxybutyrate/polycaprolactone Nanocomposites. *Sci. World J.* **2014**, *2014*, 1–9.

(54) Ritger, P. L.; Peppas, N. A. A simple equation for description of solute release II. Fickian and anomalous release from swellable devices. *J. Controlled Release* **1987**, *5* (1), 37–42.

(55) Baek, N.; Lee, J.; Park, K. Aqueous N, N-Diethylnicotinamide (DENA) Solution as a Medium for Accelerated Release Study of Paclitaxel. **2004**, *15* (4), 527–542.

(56) Sanghvi, R.; Evans, D.; Yalkowsky, S. H. Stacking Complexation by Nicotinamide: A Useful Way of Enhancing Drug Solubility. *Int. J. Pharm.* **2007**, *336* (1), 35–41.

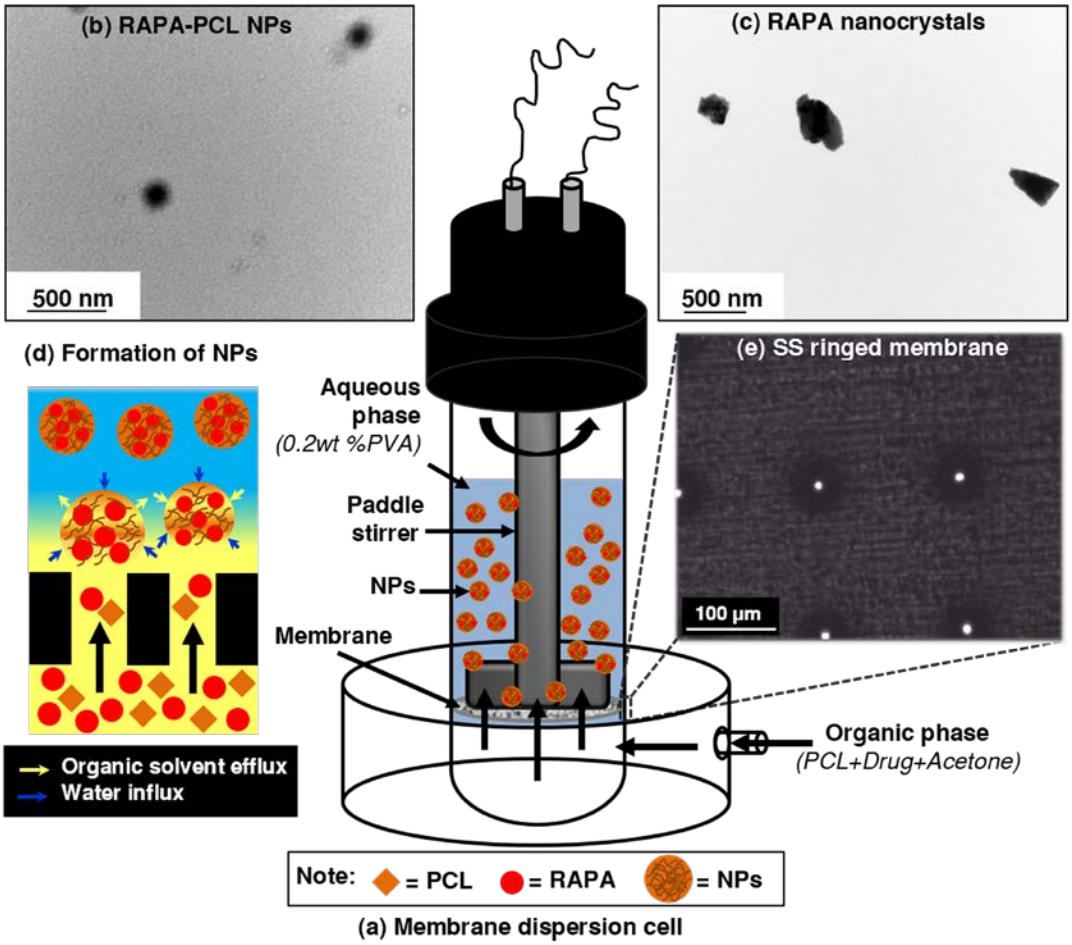

For Table of Contents Only

126.4 x 142.6 mm (300 x 300 DPI)